

$^{98}\text{Mo}(p, d)^{97}\text{Mo}$  reaction and core coupling in  $^{97}\text{Mo}$  and  $^{97}\text{Nb}^\dagger$ 

P. K. Bindal, D. H. Youngblood, and R. L. Kozub\*

*Cyclotron Institute and Physics Department, Texas A&M University, College Station, Texas 77843*

P. H. Hoffmann-Pinther

*Physics Department, Ohio University, Athens, Ohio 45701*

(Received 14 April 1975).

The  $^{98}\text{Mo}(p, d)^{97}\text{Mo}$  reaction has been used at a bombarding energy of 38.6 MeV to populate neutron hole states of  $^{97}\text{Mo}$ . Excitation energies and angular distributions were measured for levels up to 4.5 MeV in excitation. A distorted-wave-Born-approximation analysis was used to make  $l$  assignments and to obtain spectroscopic factors. Three distinct groups of weakly excited levels, one corresponding to  $l=4$  and two corresponding to  $l=1$ , were observed lying above 2.7 MeV excitation. A hole-core-coupling model is used to predict the properties of  $^{97}\text{Mo}$  and  $^{97}\text{Nb}$  and good agreement with the experiment is obtained.

NUCLEAR REACTIONS, NUCLEAR STRUCTURE  $^{98}\text{Mo}(p, d)$ ,  $E=38.6$  MeV; measured  $\sigma(\theta)$ ,  $^{97}\text{Mo}$  levels; deduced  $l$ ,  $S$ ; calculated  $J$ ,  $\pi$ ,  $S$ , particle-core-coupling model,  $Q$  for  $^{98}\text{Mo}$  ( $2^+$ ) and  $^{97}\text{Mo}$  (g.s.),  $B(E2)$ ,  $B(M1)$  for  $^{97}\text{Mo}$ ,  $^{97}\text{Nb}$ .

## I. INTRODUCTION

Recently we have studied proton and neutron hole configurations of several odd- $A$  nuclei in the  $A=90-100$  region. The study of proton hole states using the  $^{96,98,100}\text{Mo}(d, ^3\text{He})^{95,97,99}\text{Nb}$  reactions<sup>1</sup> revealed that in the Mo ground states the  $2p_{1/2}$  and  $2p_{3/2}$  orbitals were not completely filled, the  $1g_{9/2}$  subshell was about 25% filled, and there was a small occupation of the  $2d_{5/2}$  orbital. There was little change in the proton configuration as more neutrons were added above the  $1g_{9/2}$  neutron orbit. We used a hole-core-coupling model<sup>2</sup> for the  $^{95,97,99}\text{Nb}$  isotopes,<sup>1,3</sup> where the  $0^+$  ground state and the first  $2^+$  state of the neighboring even-even Mo nuclei were coupled to the  $2p_{1/2}$ ,  $2p_{3/2}$ , and  $1f_{5/2}$  shell-model orbits to predict the proton hole states. This simple model predicted energy spectra and spectroscopic factors in fair agreement with the experimental results. In the present study, we used this model to predict the structure of  $^{97}\text{Mo}$ . In a later communication we shall present results of the hole-phonon model where effects of dissociation of phonons into particle-hole pairs will be included.<sup>4</sup>

The level structure of  $^{97}\text{Mo}$  has been calculated by Vervier<sup>5</sup> and by Choudhury and Clemens.<sup>6</sup> Vervier uses the effective mutual interaction of the nucleons in the  $\pi(2p_{1/2})^2\pi(1g_{9/2})^2\nu(2d_{5/2})^{-1}$  configuration outside the  $^{88}\text{Sr}$  core, whereas Choudhury and Clemens couple a  $\nu d_{5/2}$  hole to the quadrupole vibrations of the  $^{98}\text{Mo}$  core, truncating the core space to include the contributions up to three phonon excitations. Because of this, they ignore

contributions from the  $3s_{1/2}$ ,  $2d_{3/2}$ ,  $1g_{7/2}$ , and  $1g_{9/2}$  neutron orbits so the predicted spectroscopic factors for neutron pickup reactions are nonzero only for  $\frac{5}{2}^+$  levels, whereas experimental studies show that there is significant strength for  $l=0$  and  $l=4$  states. Information on the levels of  $^{97}\text{Mo}$  is compiled in Ref. 7.

The  $^{98}\text{Mo}(p, d)^{97}\text{Mo}$  reaction was studied to obtain additional nuclear structure information about the  $^{98}\text{Mo}$  and  $^{97}\text{Mo}$  nuclei. The experimental procedure and data analysis technique is outlined in the next section, followed by a brief discussion of the experimental results obtained and the distorted-wave-Born-approximation (DWBA) analysis in Sec. III. In Sec. IV, we present a comparison of the energy levels,  $J^\pi$  values, and spectroscopic factors predicted by the hole-core-coupling model with the experimental data. Also, the calculated transition probabilities and quadrupole moments are compared with the experimental results.

## II. EXPERIMENTAL PROCEDURE AND DATA ANALYSIS

The experimental details are similar to those described previously.<sup>8</sup> A 38.6 MeV proton beam from the Texas A&M cyclotron was used to bombard a self-supporting Mo foil enriched to 97.1% in  $^{98}\text{Mo}$ . The target thickness, determined by weighing, was 0.550 mg/cm<sup>2</sup>. Two silicon detector telescopes spaced 5° apart were used simultaneously to reduce data acquisition time, and selected data points were checked by measurement with both systems. The telescopes consisted of 500  $\mu\text{m}$  ( $\Delta E$ ), 3 mm ( $E$ ), and 1.5 mm

(veto) detectors for the forward stack and 200  $\mu\text{m}$  ( $\Delta E$ ), 1 mm ( $E$ ), and 700  $\mu\text{m}$  (veto) detectors for the other stack. The veto detector served to eliminate pulses due to the elastically scattered protons. The over-all resolution obtained was about 50 keV full width at half-maximum. A typical deuteron spectrum is shown in Fig. 1. The actual spectra extend up to an excitation of about 17 MeV, sufficient to obtain information on the isobaric analog states, the subject of a previous communication.<sup>9</sup> Angular distributions were obtained for 39 groups kinematically identified with this reaction for laboratory angles from 7.5° to 42.5°.

Due to the high density of levels special considerations were required for extraction of level parameters. An interactive peak-fitting computer code which permitted fitting up to nine Gaussian peaks simultaneously after subtraction of background was used for data analysis. During display of a spectrum on the 25.4 cm display oscilloscope initial guesses for the number of peaks, their position and heights, are entered with the aid of a "moving dot" and then a search on values on any or all of these parameters (choice controlled by operator) is performed to minimize  $\chi^2$  for the data region selected. The resulting fit is displayed with the data for immediate evaluation. Unsatis-

factory fits are discarded; the parameters for satisfactory fits are both printed out and stored on tape (after conversion to cross section, excitation energy, etc.). Several criteria were used to enhance the reliability of these fits. Since all of the levels are bound, the peak shape and width should remain the same over the range of interest; hence all peaks were required to conform in shape and width to the ground state. All peaks counted as real (Table I) appeared at essentially all angles within  $\pm 20$  keV excitation energy. In several places weak peaks were required to fit data at a few angles only. These are not listed. The background was chosen for a given region as consistently as possible for different angles. A sample fit to the region from 1.83–2.26 MeV is shown in Fig. 2.

### III. DISTORTED-WAVE BORN APPROXIMATION AND EXPERIMENTAL RESULTS

#### A. DWBA parameters

Distorted-wave-Born-approximation (DWBA) calculations, including finite range and nonlocal (FRNL) corrections, were performed using the computer code DWUCK.<sup>10</sup> Optical model parameters and the FRNL parameters are listed in Table II. The calculated and experimental cross sections

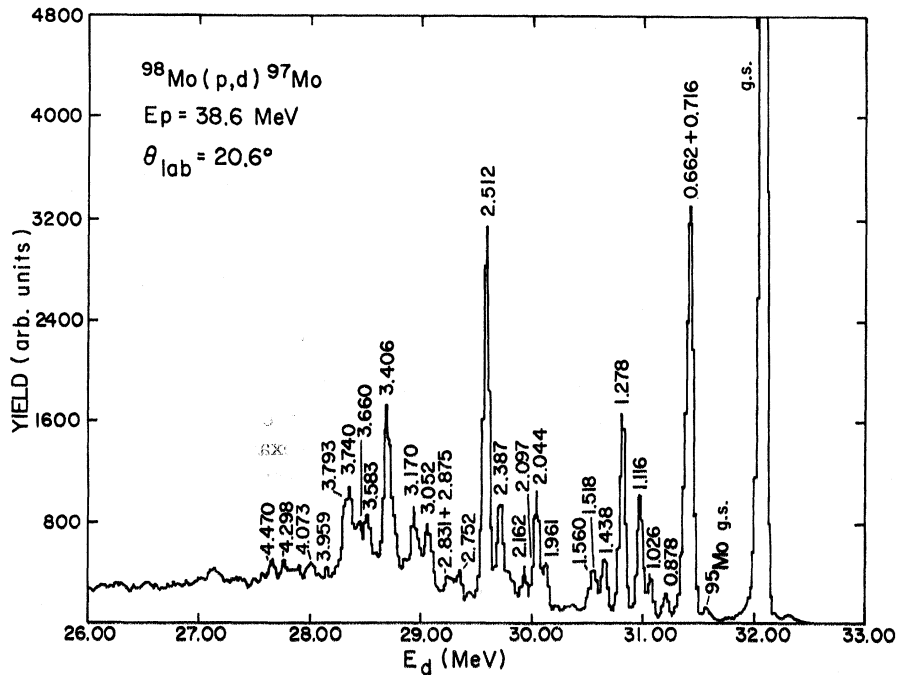


FIG. 1. A spectrum of the  $^{98}\text{Mo}(p, d)^{97}\text{Mo}$  reaction. The excitation energies of observed states are indicated in MeV. Some of the weak states at this angle are not indicated.

TABLE I. Summary of experimental results for  $^{97}\text{Mo}$ .

$^{97}\text{Mo}^*$ (MeV $\pm$ keV)	$l_n$	$J^\pi$ <sup>a</sup>	Present work	$C^2S_n$		Coulomb excitation <sup>d</sup>		Nuclear data <sup>e</sup>	
				$(d, t)$ <sup>b</sup> $E_d = 15$ MeV	$(d, t)$ <sup>c</sup> $E_d = 23$ MeV	$E_x$ (keV)	$J^\pi$	$E_x$ (keV)	$J^\pi$
0.0	2	$\frac{5}{2}^+$	2.6	5.82	2.1	0.0	$\frac{5}{2}^+$	0.0	$\frac{5}{2}^+$
						480.9	$\frac{3}{2}^+$	480.9	$\frac{3}{2}^+$
0.662 $\pm$ 10	4	$\frac{7}{2}^+$	0.48			658.2	$\frac{7}{2}^+$	657.92	$\frac{7}{2}^+$
	0	$\frac{1}{2}^+$	0.40	0.79 <sup>f</sup>	(0.3)	679.6	$\frac{1}{2}^+$	679.6	$(\frac{1}{2}^+)$
0.716 $\pm$ 10	2	$\frac{5}{2}^+$	0.32		(0.2)	719.3	$\frac{5}{2}^+$	719.47	$(\frac{3}{2}, \frac{5}{2})^+$
						721.1	$(\frac{3}{2}^+)$	721.1	$(\frac{1}{2}, \frac{3}{2}, \frac{5}{2})^+$
0.878 $\pm$ 7	0	$\frac{1}{2}^+$	0.04	0.082		881.1	$\frac{1}{2}^+$	888.2	$\frac{1}{2}^+$
1.026 $\pm$ 7	4	$\frac{7}{2}^+$	0.20			1024.6	$\frac{7}{2}^+$	1024.53	$\frac{7}{2}^+$
1.116 $\pm$ 7	2	$\frac{3}{2}^+$	small <sup>g</sup>		0.2	1092.6	$\frac{3}{2}^+$	1092.6	$(\frac{3}{2}, \frac{5}{2})^+$
	4	$\frac{9}{2}^+$	0.44			1116.7	$\frac{9}{2}^+$	1116.7	$\frac{9}{2}^+$
								1136.0	
								1148.6	
1.278 $\pm$ 8	4	$\frac{7}{2}^+$	small <sup>g</sup>			1268.8	$\frac{7}{2}^+$	1268.63	$\frac{7}{2}^+$
	2	$\frac{3}{2}^+$	0.47	0.61	0.4	1284.6	$(\frac{3}{2}^+)$	1273.0	$(\frac{3}{2}, \frac{5}{2})^+$
								1284.0	$(\frac{13}{2}^+)$
								1409.5	$(\frac{11}{2}^+)$
1.438 $\pm$ 7	5	$\frac{11}{2}^-$	0.3					1437.3	$(\frac{11}{2}^-)$
	2	$\frac{3}{2}^+$	small <sup>g</sup>					1447.0	$(\frac{3}{2}, \frac{5}{2})^+$
1.518 $\pm$ 10	4	$\frac{9}{2}^+$	0.14			1515.5	$\frac{9}{2}^+$	1515.64	$(\frac{7}{2}, \frac{9}{2})^+$
								1545.2	$(\frac{5}{2}, \frac{7}{2})^-$
1.560 $\pm$ 10	2	$\frac{3}{2}^+$	0.05					1565.1	
	3	$\frac{5}{2}^-$	small <sup>g</sup>						
								(1629.13)	
								1741.0	$(\frac{3}{2}, \frac{5}{2})^+$
								1780.0	
								(1858.0)	
								1921.3	$(\frac{13}{2}^+)$
1.961 $\pm$ 8	2	$\frac{3}{2}^+$	0.03						
	4	$\frac{7}{2}^+$	0.12						
								2002.0	$(\frac{15}{2}^-)$
								2010.0	$(\frac{7}{2}, \frac{9}{2})^+$
2.044 $\pm$ 9	4	$\frac{7}{2}^+$	0.61					2065.0	$\frac{1}{2}^+$
	0	$\frac{1}{2}^+$	small <sup>g</sup>	0.059					
2.097 $\pm$ 12	1	$\frac{1}{2}^-$	0.035						
2.162 $\pm$ 9	2	$\frac{3}{2}^+$	0.08	0.248				2153.0	$(\frac{3}{2}, \frac{5}{2})^+$
2.267 $\pm$ 12	1	$\frac{1}{2}^-$	0.08					2160.0	
								(2284.0)	
2.320 $\pm$ 12	(4)	$(\frac{9}{2}^+)$	(0.12)					(2325.0)	
2.387 $\pm$ 9	1	$\frac{1}{2}^-$	0.39		0.4			2388.0	$(\frac{1}{2}, \frac{3}{2})^-$
								2435.0	$(\frac{13}{2}^+)$
								2480.0	$(\frac{7}{2}, \frac{9}{2})^+$
2.512 $\pm$ 10	4	$\frac{9}{2}^+$	1.6		1.5			2500.0	$(\frac{7}{2}, \frac{9}{2})^+$
								(2552.0)	

TABLE I (Continued)

$^{97}\text{Mo}^*$ (MeV $\pm$ keV)	$l_n$	$J^\pi$ <sup>a</sup>	Present work	$C^2S_\pi$ ( $d, t$ ) <sup>b</sup>		Coulomb excitation <sup>d</sup>		Nuclear data <sup>e</sup>	
				$E_d = 15$ MeV	$E_d = 23$ MeV	$E_x$ (keV)	$J^\pi$	$E_x$ (keV)	$J^\pi$
2.752 $\pm$ 12	1	$\frac{1}{2}^-$	0.15					(2561.0)	
2.831 $\pm$ 15	1	$\frac{1}{2}^-$	0.06		0.2			2830.0	$(\frac{1}{2}, \frac{3}{2})^-$
2.875 $\pm$ 15	1	$\frac{1}{2}^-$	0.06						
3.004 $\pm$ 15	1	$\frac{1}{2}^-$	0.15						
3.052 $\pm$ 15	1	$\frac{1}{2}^-$	0.26						
3.111 $\pm$ 20	1	$\frac{1}{2}^-$	0.16						
3.170 $\pm$ 15	4	$\frac{9}{2}^+$	0.30						
	1	$\frac{1}{2}^-$	0.06						
3.260 $\pm$ 20	1	$\frac{1}{2}^-$	0.13						
3.345 $\pm$ 20	1	$\frac{1}{2}^-$	0.20						
3.406 $\pm$ 15	4	$\frac{9}{2}^+$	0.75						
3.519 $\pm$ 20	2	$\frac{3}{2}^+$	0.07						
3.583 $\pm$ 15	4	$\frac{9}{2}^+$	0.37						
3.660 $\pm$ 20	4	$\frac{9}{2}^+$	0.29						
3.740 $\pm$ 20	4	$\frac{9}{2}^+$	0.39					(3749.0)	
3.793 $\pm$ 20	4	$\frac{9}{2}^+$	0.17						
	1	$\frac{3}{2}^-$	0.07						
3.959 $\pm$ 25	1	$\frac{3}{2}^-$	0.10						
4.073 $\pm$ 25	1	$\frac{3}{2}^-$	0.08						
4.254 $\pm$ 25	1	$\frac{3}{2}^-$	0.13						
4.298 $\pm$ 25	1	$\frac{3}{2}^-$	0.08						
4.423 $\pm$ 25	1	$\frac{3}{2}^-$	0.01						
4.470 $\pm$ 25	1	$\frac{3}{2}^-$	0.09						
3.95 - 4.54	1	$\frac{3}{2}^-$	0.68						

<sup>a</sup>  $J^\pi$  values are those which seem plausible on a shell model basis; no assignments have been made.

<sup>b</sup> Reference 14.

<sup>c</sup> Reference 20.

<sup>d</sup> Reference 13.

<sup>e</sup> Reference 7.

<sup>f</sup> The 0.662 MeV and 0.716 MeV levels were not resolved (Ref. 14).

<sup>g</sup> A mixture of two  $l$  transfers was tried as such levels are known within 20 keV. The data could be fitted by a single  $l$  transfer although there may be a small contribution from the other  $l$  transfer.

are related by

$$\left(\frac{d\sigma}{d\Omega}\right)_{\text{exp}} = \frac{NC^2S}{2J+1} \left(\frac{d\sigma}{d\Omega}\right)_{\text{DW}}, \quad (1)$$

where  $J$  is the transferred angular momentum,  $N$  is the normalization constant determined from the internal structure of the projectile, and  $C^2S$  is the spectroscopic factor. We have used a value of  $N = 2.54$  in the present work.

## B. Experimental results

In Table I, we compare the energy spectrum obtained in the present study with the previously available information<sup>7</sup> which extends only up to 3 MeV in excitation. For the purpose of clarity, we have separated the published information into three parts, the first obtained by pickup reactions to compare spectroscopic factor information, the

TABLE II. Optical model and FRNL parameters used in DWBA calculations (MeV Fm units)

Particle	$V$	$r_0$	$a$	$W$	$4W_D$	$r_I$	$a_I$	$r_c$	$V_{so}$	$r_{so}$	$a_{so}$	$\beta^a$	FRNL <sup>b</sup>
$p^c$	48.67	1.17	0.75	5.84	15.24	1.32	0.61	1.3	24.8	1.01	0.75	0.85	0.695
$d^d$	100.8	1.099	0.835		53.64	1.344	0.747	1.3	6.53	1.099	0.835	0.54	
$n$		1.15	0.65			$\lambda_{so} = 25$		1.25				0.85	

<sup>a</sup> Nonlocal parameters used in DWUCK.

<sup>b</sup> Finite range parameters for ( $p, d$ ) reaction used in DWUCK.

<sup>c</sup> Reference 11.

<sup>d</sup> Reference 12.

second containing levels observed in a recent Coulomb excitation experiment<sup>13</sup> to use information about  $J^\pi$  assignments, and the third containing all the adopted levels by Medsker<sup>7</sup> based on the information available in the literature. A weak peak seen at  $495 \pm 6$  keV is close to the position of the first excited state (480.9 keV). However, the peak is primarily due to the <sup>95</sup>Mo ground state (the target contained 2% <sup>96</sup>Mo). Our excitation energies and spectroscopic factors for low-lying levels are in excellent agreement with others as shown in Table I, except for the absence of the 1.71 and 1.78 MeV levels which were observed in the ( $d, t$ ) reaction by Hjorth and Cohen.<sup>14</sup> The 1.71 MeV level has not been observed in any other study and the 1.78 MeV level is also questionable. These levels might have been due to an impurity in their targets (they were backed by Cu foil).

The angular distributions and corresponding DWBA predictions are shown in Figs. 3–6. Fits are satisfactory for most of the levels. The state at 0.662 MeV is not fitted by assuming a unique  $l$  transfer. States assigned as  $\frac{7}{2}^+$  and  $\frac{1}{2}^+$  are observed in Coulomb excitation studies within 15 keV of this energy. The angular distribution for this state could be fitted assuming it was a doublet populated by  $l=0$  and  $l=4$  transfers. Here we have

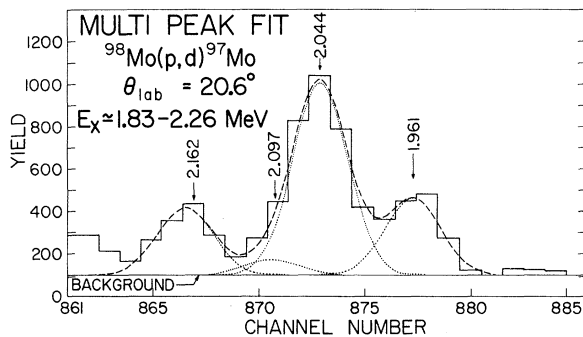


FIG. 2. Multipipeak fit for the region from 1.83–2.26 MeV. The 2.097 MeV level is very weakly excited at this angle. The dotted lines indicate individual peaks, while the dashed line shows the over-all fit.

taken the experimental shape of  $l=0$  angular distribution from the known  $l=0$  level at 0.878 MeV, as the DWBA prediction did not fit its angular distribution satisfactorily. A state at  $1.560 \pm 0.020$  MeV excitation has been assigned  $l=3$  in the ( $d, p$ ) and ( $p, d$ ) studies.<sup>14,15</sup> In the present work, the angular distribution for this state is fitted by  $l=2$  transfer. For comparison, the DWBA prediction for an  $l=3$  transfer is also shown. Angular distributions for most of the other states could be fitted satisfactorily by assuming a unique  $l$  value; however, a few of the states needed a mixture of two  $l$  transfers as shown in Figs. 3–6. These mixings are consistent with the available information as shown in Table I.

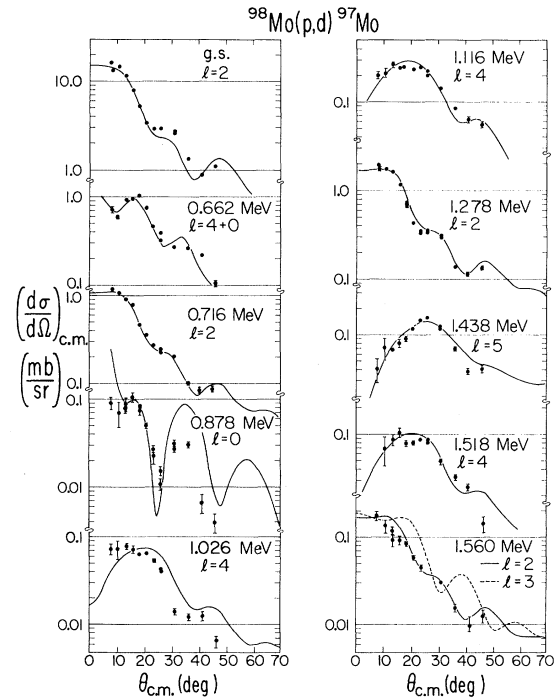


FIG. 3. Angular distributions for the <sup>98</sup>Mo( $p, d$ )<sup>97</sup>Mo reaction (g.s.–1.560 MeV). The errors shown are statistical only. The curves are DWBA calculations for the  $l$  transfers indicated.

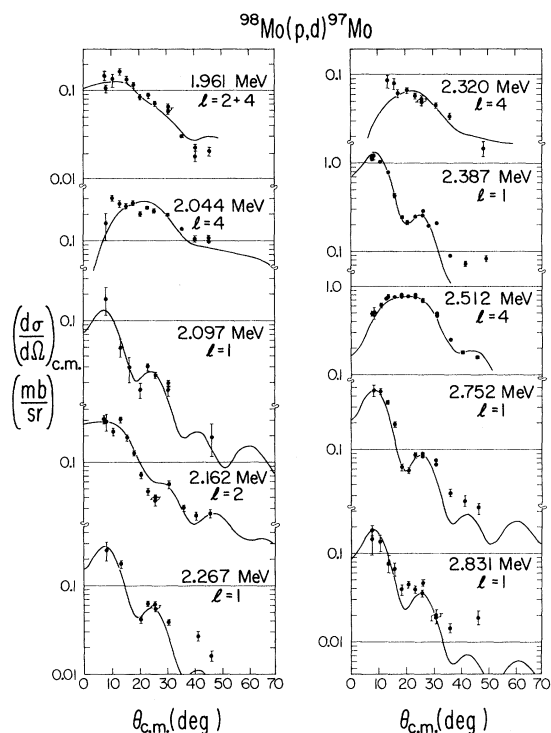


FIG. 4. Angular distributions for the  $^{98}\text{Mo}(p, d)^{97}\text{Mo}$  reaction (1.961–2.831 MeV). See Fig. 3 caption.

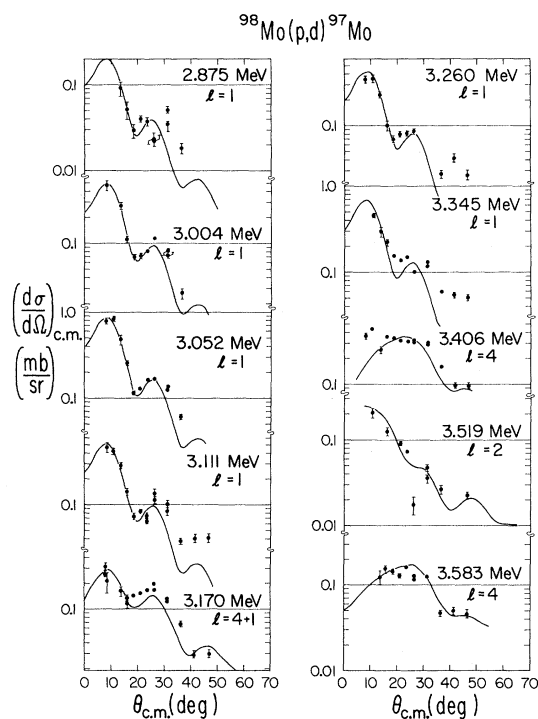


FIG. 5. Angular distributions for the  $^{98}\text{Mo}(p, d)^{97}\text{Mo}$  reaction (2.875–3.583 MeV). See Fig. 3 caption.

One interesting aspect of the present work is that the states above 2.7 MeV form three groups of levels; the first ranging from 2.7 to 3.3 MeV, corresponding primarily to  $l=1$  transfer; the second ranging from 3.4 to 3.8 MeV with mostly an  $l=4$  transfer; the third from 3.9 to 4.5 MeV, fitted with an  $l=1$  transfer. The spectroscopic factors for individual states are small, but the groups were resolved very nicely. Although assignments for a few of the weak states may not be definite, the over-all splitting of the levels into three distinct groups is apparent. The angular distribution for the aggregate of levels in the region of 3.9 to 4.5 MeV, along with the DWBA prediction for  $l=1$  transfer, is seen in Fig. 6.

Most of the observed  $2d_{5/2}$  and  $3s_{1/2}$  strength is in the ground and the 0.662 MeV states, respectively, of  $^{97}\text{Mo}$ . As no spin assignments were made, definitive allocation of  $l=2$  and 4 strengths to the  $2d_{3/2}$ ,  $1g_{7/2}$ , and  $1g_{9/2}$  orbitals could not be made; however, the in-beam spectroscopy and Coulomb excitation results show  $\frac{7}{2}^+$  and  $\frac{9}{2}^+$  states that correspond to levels observed here. The strong  $l=4$  level at 2.51 MeV probably contains most of the  $1g_{9/2}$  strength. A significant mixing of the  $3s_{1/2}$ ,  $2d_{3/2}$ , and  $1g_{7/2}$  orbits appears to be present in the ground state of  $^{98}\text{Mo}$ , and a small admixture of  $1h_{11/2}$  orbit is also observed. The

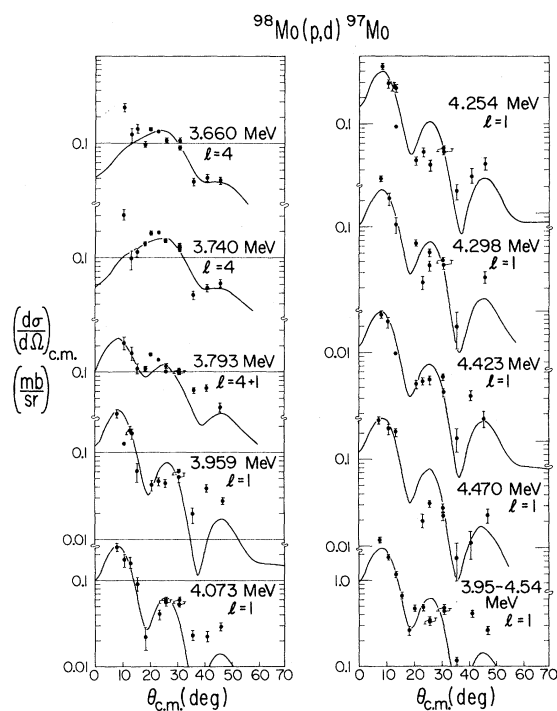


FIG. 6. Angular distributions for the  $^{98}\text{Mo}(p, d)^{97}\text{Mo}$  reaction (3.660–4.470 MeV). See Fig. 3 caption.

largest component is the  $2d_{5/2}$ . Many levels corresponding to  $l=1$  transfer are observed but the total strength for the  $2p_{1/2}$  and  $2p_{3/2}$  orbits is not exhausted. The remainder of the  $2p$  and  $1g_{9/2}$  orbital strength is expected to lie in higher unresolved levels along with the  $1f_{5/2}$  strength which is not observed in the present study.

#### IV. STRUCTURE CALCULATIONS WITH THE PARTICLE-CORE COUPLING MODEL

##### A. Parameters of the model

As discussed in the Introduction, there are two previous calculations<sup>5,6</sup> of the structure of  $^{97}\text{Mo}$ . Since these authors include only  $\nu(d_{5/2})^{-1}$  in their calculations, a meaningful comparison with the data is not possible as the experimental information reveals a more complicated situation. Recently we used a particle-core model<sup>2</sup> to predict the proton-hole states of odd- $A$  Nb isotopes<sup>1,3</sup> with fair agreement with the experimental data. In this model, the single-particle states are coupled with the ground state and low-lying excited states of the core. We use this simple model to predict the neutron-hole states of  $^{97}\text{Mo}$  with  $^{98}\text{Mo}$  as the core. The total Hamiltonian  $H$  for the odd-mass nucleus is written as

$$H = H_0 + H_{\text{sp}} + H_{\text{int}}, \quad (2)$$

where  $H_0$  is the core Hamiltonian,  $H_{\text{sp}}$  the single-particle Hamiltonian for the extra nucleon, and  $H_{\text{int}}$  describes the interaction between the extra nucleon and the core. In the present work, we have taken the interaction as

$$H_{\text{int}} = \xi(j_c^{(1)} \cdot j_p^{(1)}) + \eta(Q_c^{(2)} \cdot Q_p^{(2)}), \quad (3)$$

where  $j$  and  $Q$  are the angular momentum and mass quadrupole moment operators, respectively. The parameter  $\xi$  is the strength of the dipole-dipole interaction. In practice, if one includes only two states of the core, i.e., the ground state and the first  $2^+$  state, one introduces two different parameters, namely,  $\chi_1$ , defined as  $\eta(0 || Q_c || 2)$  and  $\chi_2$ , defined as  $\eta(2 || Q_c || 2)$ . These two parameters are directly related to the  $B(E2)$  transition probability for the  $0^+$  ground state to the first  $2^+$  state and the quadrupole moment of the  $2^+$  state of the core. Using self-consistent arguments, one can calculate the strength of the  $Q \cdot Q$  term, which together with the reduced matrix element of  $Q_c$  yields

$$\chi_1 = \frac{4\pi}{3} \frac{\hbar^2}{m r_0^2} \nu^2 A^{-5/3} \frac{A}{Z} [B(E2; 0^+ - 2^+)]^{1/2}. \quad (4)$$

Here  $\nu$  is the oscillator parameter given by

$$\nu = 41M/\hbar^2 A^{1/3}. \quad (5)$$

TABLE III. Quasiparticle energies and occupancy numbers used in the calculations for  $^{97}\text{Mo}$ .

State	Energy (MeV)	$\nu^2$
$3s_{1/2}$	1.0	0.29
$2d_{3/2}$	2.5	0.16
$2d_{5/2}$	0.0	0.60
$1g_{7/2}$	1.0	0.17
$1g_{9/2}$	3.2	0.95

The factor  $A/Z$  in Eq. (4) arises as the parameter  $\chi_1$  is defined by a mass quadrupole moment operator. Using the rotational model wave functions, one can show easily that the ratio of  $\chi_2/\chi_1$  is given by

$$\frac{\chi_2}{\chi_1} = \frac{\langle 2 || Q_c || 2 \rangle}{\langle 2 || Q_c || 0 \rangle} = -\left(\frac{10}{7}\right)^{1/2}$$

for a prolate shape. The vibrational model would predict this ratio to be zero. This indicates that the value of  $\chi_2$  should lie between 0.0 and  $1.195\chi_1$ , the sign of  $\chi_2$  indicating a prolate (negative  $\chi_2$ ) or an oblate (positive  $\chi_2$ ) shape.

The excitation energies and the wave functions of  $^{97}\text{Mo}$  were obtained by diagonalizing the total Hamiltonian. The positive parity levels  $\frac{1}{2}^+$ ,  $\frac{3}{2}^+$ ,  $\frac{5}{2}^+$ ,  $\frac{7}{2}^+$ ,  $\frac{9}{2}^+$ ,  $\frac{11}{2}^+$ , and  $\frac{13}{2}^+$  of  $^{97}\text{Mo}$  were assumed to be given by the coupling of neutron orbits in the  $3s_{1/2}$ ,  $2d_{3/2}$ ,  $2d_{5/2}$ ,  $1g_{7/2}$ , and  $1g_{9/2}$  subshells with the  $0^+$  ground state and the first  $2^+$  excited state of  $^{98}\text{Mo}$ . Since the spectroscopic information indicates that these orbits are not completely filled, a quasiparticle formalism was used in the calculation. Quasiparticle energies and occupancy numbers used in the calculation are shown in Table III. We expect the  $1g_{9/2}$  state to be almost filled, so its occupancy number is taken as 0.95 although only about half of its strength is observed. The Hamiltonian matrices for these states were diagonalized to obtain the energy eigenvalues and eigenfunctions for values of  $\chi_1$  from 0.0 to 0.5 and  $\chi_2$  from  $-0.5$  to  $0.5$ . The best agreement with the experimental data was obtained with the value of  $\chi_1 = 0.34 \text{ MeV fm}^{-2}$  obtained from Eq. (4), where the value of  $B(E2; 0 - 2)$  for  $^{98}\text{Mo}$  was taken from Ref. 16. The values of  $\chi_2$  and  $\xi$  for the best agreement were found to be  $-0.24 \text{ MeV fm}^{-2}$  and  $-0.05 \text{ MeV}$ , respectively. This indicates that the strength of the  $j \cdot j$  term is weak and the shape of  $^{98}\text{Mo}$  is prolate.

##### B. Energy spectra and spectroscopic factors

Theoretical and experimental results for  $^{97}\text{Mo}$  are shown in Fig. 7. The calculations predict

three  $\frac{1}{2}^+$  levels; the first two are in reasonably good agreement with the data, while the third is predicted to be about 1 MeV higher than the known  $\frac{1}{2}^+$  level at 2.065 MeV. The predicted energies and spectroscopic factors for low-lying  $l=2$  levels are in good agreement with the data. The theory predicts a  $\frac{3}{2}^+$  level at 0.49 MeV which might correspond to the  $\frac{3}{2}^+$  level at 0.48 MeV observed in studies other than one-particle transfer reaction work. An  $l=2$ , presumably  $\frac{3}{2}^+$  level at 1.23 MeV is not predicted in the present work. The predicted levels for  $l=4$  are in good agreement with the experimental results for low-lying states. A weak  $l=4$ ,  $J=\frac{9}{2}$  level at 1.53 MeV is not predicted by the theory at this energy. The spectroscopic factor for the 2.5 MeV level is predicted to be too large.

The over-all agreement with the low-lying positive parity states is good, bearing in mind that this is a simple model. The number of states that can be predicted with the inclusion of only the  $0^+$  ground state and the first  $2^+$  state of the core is limited. The inclusion of higher states of the core, which would fragment the strength into ad-

ditional states, would introduce more parameters in the present model. However, the necessity of this is further emphasized by the spread of  $l=1$  strength among many states in this nucleus. In addition, the strength of the  $\frac{9}{2}^+$  state predicted to be at 4.8 MeV in our model would be shared by other groups of states in this high energy region. This is borne out in the work of Ishimatsu *et al.*<sup>15</sup>

### C. Transition probabilities and quadrupole moments

The spectroscopic factors are good checks on the single-particle component of the wave functions. The other components of the wave functions can be checked by calculating the quadrupole moment of the ground state of  $^{97}\text{Mo}$  and the transition probabilities. The theory predicts 0.236 eb for the quadrupole moment of the  $\frac{5}{2}^+$  ground state of  $^{97}\text{Mo}$ . There are two experimental values known which are  $(0.15 \pm 0.04)$  eb<sup>17</sup> and  $(1.1 \pm 0.2)$  eb.<sup>18</sup> Choudhury and Clemens<sup>6</sup> predict it to be 0.525 eb and Kisslinger and Sorensen<sup>19</sup> predict 0.36 eb for this quantity. Our predicted value is close to the more recent experimental value of Pendlebury and Ring.<sup>17</sup> The effective spin gyromagnetic factor is taken to be  $g_s^{\text{eff}} = 0.58 \times g_s^{\text{free}}$  from Choudhury and Clemens. Using  $g_l^{\text{eff}} = 0.0$ , the predicted magnetic moment (in units of  $e\hbar/2Mc$ ) of the ground state is  $-1.044$ , which is in agreement with the experimental value  $(-0.9208)$ <sup>7</sup> and in reasonable agreement with the calculated value of Choudhury and Clemens  $(-0.878)$ .

Some of the calculated  $B(E2)$  and  $B(M1)$  values are compared in Table IV with the recent values of Barrette *et al.*<sup>13</sup> Although the transition probabilities are in reasonable agreement with the experimental data, the transitions involving  $\frac{5}{2}^+$  states are not reproduced very well. We are, at present, in the process of calculating the structure of odd-A systems by including higher phonons and the Pauli principle.<sup>4</sup> The inclusion of the Pauli principle is known to reduce the collectivity which would alter the transition probabilities.

Using the experimental value<sup>16</sup> of the transition probability  $B(E2; 0^+ \rightarrow 2^+)$  for  $^{98}\text{Mo}$  and the parameters  $\chi_1$  and  $\chi_2$  given above, one can estimate the quadrupole moment of the first  $2^+$  state of  $^{98}\text{Mo}$ . It is found to be  $-0.286$  eb, which lies between the predictions of the collective vibrational model and the rotational model. The former predicts 0.0 eb, whereas the latter model predicts  $-0.484$  eb.

### D. $^{97}\text{Nb}$

As mentioned earlier, we had used this core-coupling model for  $^{97}\text{Nb}$ . Although the over-all fit with the data was satisfactory, the  $\frac{5}{2}^-$  states

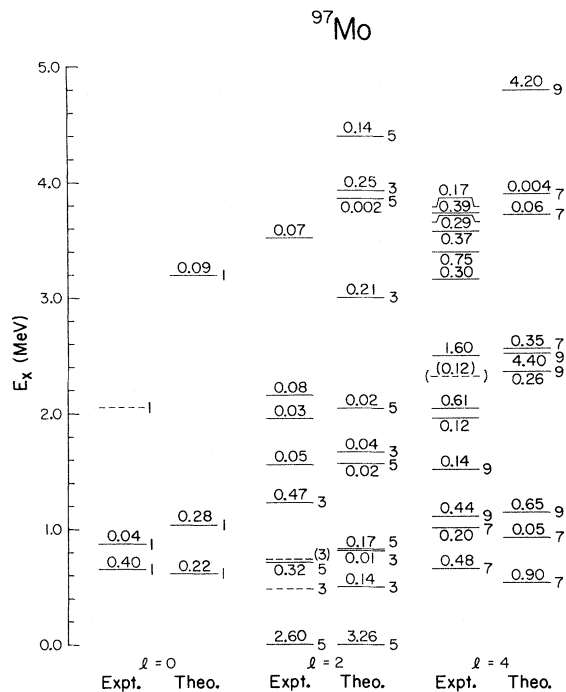


FIG. 7. Comparison of the experimentally observed  $l=0, 2$ , and  $4$  energy levels with the theoretical predictions for  $^{97}\text{Mo}$ . The experimental and calculated spectroscopic factors are indicated in the middle of the lines and the theoretical predictions and experimental assignments for  $2J$  (wherever known) are indicated on the right of the line.



TABLE IV. Transition probabilities for  $^{97}\text{Mo}$ .

Transition	$B(E2)_{\text{expt}}^a$ ( $10^{-50} e^2 \text{cm}^4$ )	$B(E2)_{\text{theo}}$ ( $10^{-50} e^2 \text{cm}^4$ )	$B(M1)_{\text{expt}}^a$ [[ $(e\hbar/2Mc)^2$ ]	$B(M1)_{\text{theo}}$ [[ $(e\hbar/2Mc)^2$ ]
$\frac{3}{2}_1^+ \rightarrow \frac{5}{2}_1^+$	$3.07 \pm 0.17$	1.07	$(2.2 \pm 0.4) \times 10^{-2}$	$3.1 \times 10^{-2}$
$\frac{7}{2}_1^+ \rightarrow \frac{3}{2}_1^+$	$7.9_{-2.9}^{+4.7}$	3.79	0.0	0.0
$\frac{7}{2}_1^+ \rightarrow \frac{5}{2}_1^+$	$0.035 \pm 0.005$	0.62	$(6.9_{-1.4}^{+2.3}) \times 10^{-2}$	$1.1 \times 10^{-3}$
$\frac{1}{2}_1^+ \rightarrow \frac{5}{2}_1^+$	$1.38 \pm 0.09$	3.10	0.0	0.0
$\frac{5}{2}_2^+ \rightarrow \frac{3}{2}_1^+$	$<4.2$ [ $<0.5$ ]	0.21	$(6.9_{-2.5}^{+5.0}) \times 10^{-2}$ $(1.3 \pm 0.3) \times 10^{-2}$	$1.4 \times 10^{-1}$
$\frac{5}{2}_2^+ \rightarrow \frac{5}{2}_1^+$	$0.39 \pm 0.03$	4.84	$(6.4_{-2.7}^{+4.7}) \times 10^{-3}$ $(1.3_{-0.7}^{+2.9}) \times 10^{-5}$	$1.3 \times 10^{-2}$
$\frac{3}{2}_2^+ \rightarrow \frac{5}{2}_1^+$	$0.252 \pm 0.023$	3.73	$(2.5_{-1.3}^{+7.3}) \times 10^{-2}$ $(1.6_{-0.7}^{+1.2}) \times 10^{-4}$	$4.8 \times 10^{-2}$
$\frac{1}{2}_2^+ \rightarrow \frac{3}{2}_1^+$	$1.8_{-0.4}^{+0.5}$	1.11	$(2.1 \pm 0.5) \times 10^{-1}$	$6.8 \times 10^{-2}$
$\frac{1}{2}_2^+ \rightarrow \frac{5}{2}_1^+$	$0.55 \pm 0.06$	1.14	0	0
$\frac{7}{2}_2^+ \rightarrow \frac{7}{2}_1^+$	$0.85_{-0.36}^{+0.58}$	0.28	$(8.0_{-3.4}^{+5.4}) \times 10^{-2}$	$1.1 \times 10^{-2}$
$\frac{7}{2}_2^+ \rightarrow \frac{3}{2}_1^+$	$1.3_{-0.8}^{+1.6}$	0.030	0	0
$\frac{7}{2}_2^+ \rightarrow \frac{5}{2}_1^+$	$3.40 \pm 0.18$	5.76	$(8.5_{-3.6}^{+7.3}) \times 10^{-2}$	$2.2 \times 10^{-2}$
$\frac{3}{2}_3^+ \rightarrow \frac{3}{2}_1^+$	$0.050_{-0.023}^{+0.064}$	0.30	$(1.3_{-0.7}^{+1.6}) \times 10^{-2}$	$6.7 \times 10^{-2}$
$\frac{3}{2}_3^+ \rightarrow \frac{5}{2}_1^+$	$0.52 \pm 0.04$	0.011	$(1.7_{-1.0}^{+1.8}) \times 10^{-2}$	$5.3 \times 10^{-2}$
$\frac{9}{2}_1^+ \rightarrow \frac{5}{2}_2^+$	$5.8 \pm 1.4$	1.10	0	0
$\frac{9}{2}_1^+ \rightarrow \frac{7}{2}_1^+$	$0.045 \pm 0.008$	0.15	$(6.5 \pm 1.2) \times 10^{-3}$	$2.2 \times 10^{-2}$
$\frac{9}{2}_1^+ \rightarrow \frac{5}{2}_1^+$	$2.74 \pm 0.19$	5.18	0	0

<sup>a</sup> Reference 13.

were not predicted very well. The value of  $\chi_1$  used in those calculations was about 40% of the value used here which is the self-consistent strength of the  $Q \cdot Q$  term. The positive value of  $\chi_2$  indicated an oblate shape for  $^{98}\text{Mo}$ . Here, we have redone the calculations for  $^{97}\text{Nb}$  using the same Hamiltonian parameters as for  $^{98}\text{Mo}$ . The structure of  $^{97}\text{Nb}$  is calculated by coupling the proton holes in the  $2p_{1/2}$ ,  $2p_{3/2}$ ,  $1f_{5/2}$ , and  $1g_{9/2}$  subshells with the  $0^+$  ground state and the first  $2^+$  state of  $^{98}\text{Mo}$ . The quasiparticle energies and occupancy numbers shown in Table V are taken from Ref. 1. The calculated structure is compared with the data in Fig. 8. The predicted excitation energies,  $J^\pi$  values, and the spectroscopic factors up to 2 MeV are in excellent agree-

ment with the experimental results. The predicted states above this energy lie higher than the experimental levels by about 0.4 to 0.5 MeV with the correct order of  $J^\pi$  values and spectroscopic factors. The energy spacing between these levels al-

TABLE V. Quasiparticle energies and occupancy numbers used in the calculations for  $^{97}\text{Nb}$ .

State	Energy (MeV)	$\nu^2$
$2p_{1/2}$	0.85	0.70
$2p_{3/2}$	1.50	0.80
$1f_{5/2}$	1.90	0.90

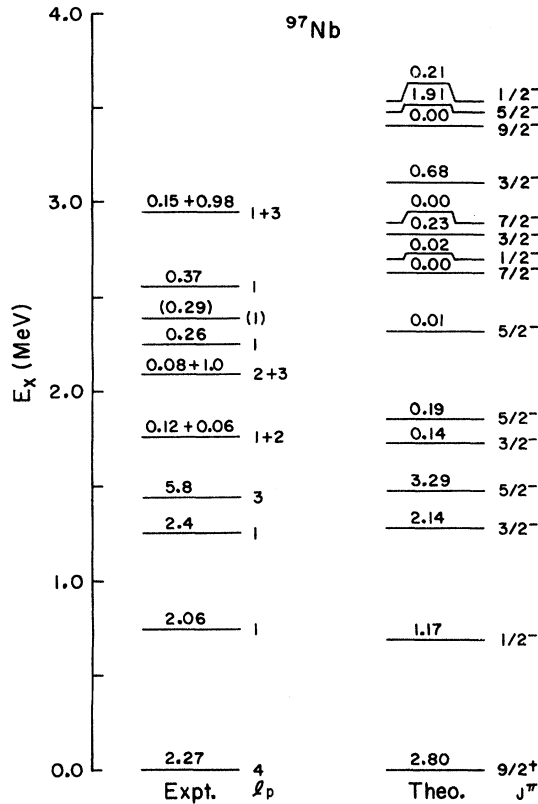


FIG. 8. Comparison of the experimental data of Ref. 1 with the theoretical predictions for  $^{97}\text{Nb}$ . See Fig. 7 caption.

so agrees with the experimental levels. Thus the parameters used in the  $^{97}\text{Mo}$  calculations also work well for  $^{97}\text{Nb}$ .

### V. CONCLUSIONS

The energy level scheme for the neutron hole states of  $^{97}\text{Mo}$  has been obtained using the  $(p, d)$

reaction. The results for the low-lying levels agree with those from other pickup studies. In addition data have been obtained for many  $l=1$  and  $l=4$  levels above 2.7 MeV in excitation. These levels form three groups, the first for  $l=1$  transfer ranging from 2.75 to 3.35 MeV, the second ranging from 3.9 to 4.5 MeV having  $l=1$  transfer. Most of the  $1d_{5/2}$  strength is observed whereas only about half of the  $1g_{9/2}$  strength is observed. Although the  $l=1$  strength is spread among many levels, only about  $\frac{1}{2}$  of the total strength for  $1p_{1/2}$  and  $1p_{3/2}$  is observed. The ground state of  $^{98}\text{Mo}$ , besides having a large  $2d_{5/2}$  strength, contains a significant admixture of the  $3s_{1/2}$ ,  $2d_{3/2}$ , and  $1g_{7/2}$  orbits along with a small admixture of  $1h_{11/2}$  shell.

A simple core-coupling model using a quasiparticle formalism was used to predict energies,  $J^\pi$  values, and the spectroscopic factors for the hole states of  $^{97}\text{Mo}$  and  $^{97}\text{Nb}$ . Good agreement with the low-lying levels is obtained. The  $l=1$  and  $l=4$  strengths are spread among many levels in high excitation energies. This model is not successful in describing these levels, which are probably of a more complicated nature, perhaps involving contributions from higher phonons. In order to investigate these effects, we are studying a hole-phonon model where the effects of dissociation of phonons into hole-particle pairs will be included. Our preliminary results are encouraging.<sup>4</sup> The predicted transition probabilities with the core-coupling model are in general higher than the experimental values. The calculated quadrupole moment of the first  $2^+$  state of  $^{98}\text{Mo}$  was found to be about 60% of the rotational limit.

The authors wish to thank Dr. T. Kishimoto for several discussions and R. Weber for his assistance in taking and analyzing the data.

<sup>†</sup>Supported in part by the National Science Foundation and the Robert A. Welch Foundation.

\*Present address: Physics Department, Queens University, Kingston, Ontario, Canada.

<sup>1</sup>P. K. Bindal, D. H. Youngblood, and R. L. Kozub, Phys. Rev. C **10**, 729 (1974).

<sup>2</sup>V. K. Thankappan and W. W. True, Phys. Rev. **137**, B793 (1965).

<sup>3</sup>P. K. Bindal and D. H. Youngblood, Phys. Rev. C **9**, 1618 (1974).

<sup>4</sup>T. Kishimoto, P. K. Bindal, and D. H. Youngblood (unpublished).

<sup>5</sup>J. Vervier, Nucl. Phys. **75**, 17 (1966).

<sup>6</sup>D. C. Choudhury and J. T. Clemens, Nucl. Phys. **A125**, 140 (1969).

<sup>7</sup>L. R. Medsker, Nucl. Data **B10**, 1 (1973).

<sup>8</sup>R. L. Kozub and D. H. Youngblood, Phys. Rev. C **4**, 535 (1971).

<sup>9</sup>R. L. Kozub and D. H. Youngblood, Phys. Rev. C **7**, 410 (1973).

<sup>10</sup>Received from P. D. Kunz, University of Colorado.

<sup>11</sup>F. D. Becchetti, Jr., and G. W. Greenlees, Phys. Rev. **182**, 1190 (1969).

<sup>12</sup>C. M. Perey and F. G. Perey, Phys. Rev. **152**, 923 (1966).

<sup>13</sup>J. Barrette, M. Barrette, R. Haroutunian, G. Lamoureux, S. Monaro, and S. Markiza, Phys. Rev. C **5**, 1376 (1972); *ibid.* **11**, 171 (1975).

<sup>14</sup>S. A. Hjorth and B. L. Cohen, Phys. Rev. **135**, B920 (1964).

<sup>15</sup>T. Ishimatsu, S. Hayashibe, N. Kawamura, T. Awaya, H. Ohmura, Y. Nakajima, and S. Mitarai, Nucl. Phys.

A185, 273 (1972).

<sup>16</sup>J. Barrette, M. Barrette, A. Boutard, R. Haroutunian, G. Lamoureux, and S. Monaro, Phys. Rev. C 6, 1339 (1972).

<sup>17</sup>J. M. Pendlebury and D. B. Ring, J. Phys. B 5, 386 (1972).

<sup>18</sup>A. Narath and D. Alderman, Phys. Rev. 143, 328 (1966).

<sup>19</sup>L. S. Kisslinger and R. A. Sorensen, Rev. Mod. Phys. 35, 853 (1963).

<sup>20</sup>H. Ohnuma and J. L. Yntema, Phys. Rev. 178, 1855 (1969).